ЖЭТФ, 2002, том 121, вып. 5, стр. 1040–1050 

# THE THEORY OF OPTICAL COMMUNICATION LINES WITH A SHORT-SCALE DISPERSION MANAGEMENT

***S. B. Medvedev**, E. G. Shapiro, M. P. Fedoruk, E. G. Turitsyna***

*Institute of Computational Technologies, Siberian Division, Russian Academy of Sciences*
*630090, Novosibirsk, Russia*

*Institute of Automation and Electrometry, Siberian Division, Russian Academy of Sciences*
*630090, Novosibirsk, Russia*

Submitted 9 November 2001

We investigate, theoretically and numerically, properties of dispersion-managed (DM) solitons in fiber lines with the dispersion compensation period $L$ much shorter than the amplification distance $Z_a$. We present the path-averaged theory of DM transmission lines with a short-scale management in the case of asymmetric maps. Applying a quasi-identical transformation, we demonstrate that the path-averaged dynamics in such systems can be described by an integrable model in some limits.

PACS: 42.65.Tg, 42.81.Dp

## 1. INTRODUCTION

Realization of the soliton-based optical data transmission has clearly demonstrated how results of the fundamental soliton theory (see, e.g., [1–12]) can be successfully used in very important practical applications. The dispersion management technique proposed recently allows the increase of the bit-rate per channel and the suppression of the interchannel interaction in WDM systems in comparison with the traditional soliton transmission [13]. The dispersion-managed (DM) soliton is a novel type of an optical information carrier with many attractive properties (see, e.g., [15–57] and references therein) combining features of the traditional fundamental soliton and the dispersion-managed non-return-to-zero transmission. The power of the DM soliton is enhanced [19] compared to the corresponding fundamental soliton. This increases the signal-to-noise ratio, reduces the Gordon–Haus jitter, and therefore improves the transmission system performance. However, in the systems (transmission regimes) limited by nonlinear pulse interactions rather than by noise, the enhanced soliton power can become a less attractive feature. For instance, the data transmission with high bit-rates of 40 Gb/s per channel and more requires a dense pulse packing, and consequently, short soliton widths. The DM soliton energy increases with the decrease of the pulse width (or in other words, with the increase of the map strength). The average power of the traditional soliton signal increases with the increase of the bit-rate (assuming the soliton width to be a fraction of the time slot) as the square of the bit-rate. For the DM soliton, this growth is even more drastic, and for short pulses, the DM soliton power can therefore become too high to be realized in practice [55]. Additionally, soliton interaction becomes an important issue as the signal power increases [55]. The energy control by the corresponding reduction of the average dispersion is limited by fluctuations of the dispersion along the fiber and by higher-order dispersive effects. Therefore, in designing soliton-based (and also general return-to-zero signal) transmission systems, the soliton power must be kept sufficiently large for the signal-to-noise ratio requirement and suppressed jitter, and at the same time, not too large to avoid the strong soliton interaction and to meet the telecommunication standards on the signal power. One way to find such an optimum for a high bit-rate DM transmission is to use a chirped-return-to-zero signal [55, 56] with less power than the DM soliton power in the corresponding system. Even though such carriers are not stable in a rigorous mathematical sense and emit radiation as they propagate, they can be successfully used in practical

*E-mail: mife@ict.nsc.ru

systems. A challenge for the soliton theory, however, is to find high-bit-rate ($\geq 40$ Gb/s per channel) transmission regimes with a truly periodic soliton-like signal propagation. The short-scale dispersion management is a means of controlling the DM soliton energy while keeping the average dispersion not too small and taking advantage of the four-wave-mixing (FWM) suppression in the WDM transmission by a high local dispersion.

The traditional dispersion management for long-haul transmission assumes the amplification distance to be much shorter than the dispersion compensation period (see, e.g., [14]). Another important application is the implementation of dispersion-compensating schemes in the existing terrestrial fiber links based on the standard monomode fibers, which typically requires rather close spacing of the dispersion compensating fibers because of the high dispersion of the standard monomode fibers at 1.55 $\mu$m. In this case, the amplification distance is typically of the order of the compensation period. The existing technologies make it possible to manufacture fibers with the continuous alternation of positive and negative dispersion sections of few kilometers long without any splicing [27]. The fundamental properties of the optical signal transmission in this regime are less studied compared to other regimes. In this paper, we investigate the optical pulse transmission in DM fiber systems with the compensation length that is much shorter than the amplification distance [41]. We examine the case of an asymmetric dispersion map. Compared to lossless models, the systems with different periods of the amplification ($Z_a$) and dispersion compensation ($L$) possess an important new degree of freedom, the parameter $L/Z_a$. A short-scale dispersion compensation ($L \ll Z_a$) leads to a reduction of the DM soliton power if we fix all system parameters and the pulse width and vary only $L/Z_a$. Below, we show that the short-scale management can be considered as a possibility of an advantageous practical realization of the weak-map regime.

## 2. THE BASIC MODEL

We first recall the basic equations and the notation. The optical pulse propagation in a cascaded transmission system with varying dispersion is governed by

$$i\frac{\partial E}{\partial z} + \frac{\lambda_0^2 D(z)}{4\pi c_l}\frac{\partial^2 E}{\partial t^2} + \frac{2\pi n_2}{\lambda_0 A_{eff}}|E|^2 E = \\ = i[-\gamma(z) + r_k \sum_{k=1}^{N} \delta(z - z_k)]E = iG(z)E, \quad (1)$$

where $z$ is the propagation distance in [km], $t$ is the retarded time in [ps], $|E|^2 = P$ is the optical power in [W], and $D(z)$ is the group velocity dispersion measured in ps/nm·km. We assume a periodic dispersion management with the period $L$, $D(z + L) = D(z)$; $z_k$ are the amplifier locations. We consider a periodic amplification with the period $Z_a$. If $\gamma = \gamma_k$ is constant between two adjacent amplifiers, then $r_k = [\exp(\gamma_k Z_a) - 1]$ is the amplification coefficient after the fiber span between the $k$-th and $(k-1)$-th amplifier, $n_2$ is the nonlinear refractive index, $A_{eff}$ is the effective fiber area, $\gamma = 0.05 \ln 10 \alpha$ (with $\alpha$ measured in dB/km) is the fiber loss of the corresponding fiber, $c_l$ is the speed of light, and $\lambda_0 = 1.55\mu$m is the carrier wavelength. We consider the general case where $L$ and $Z_a$ are rational and commensurable, namely, $nZ_a = mL = Z_0$ with integer $n$ and $m$. In this paper, we focus on the systems with the short-scale management with $n = 1$, $m > 1$, and $Z_0 = Z_a = mL$. It is customary to pass from the original optical field $E(z,t)$ to

$$A(z,t) = E(z,t) \exp\left[\int_0^z G(z')dz'\right].$$

The evolution of the scaled envelope $A$ is then given by the nonlinear Schrödinger (NLS) equation with periodic coefficients

$$iA_z + d(z)A_{tt} + \epsilon c(z)|A|^2 A = 0, \quad (2)$$

where

$$\epsilon c(z) = \frac{2\pi n_2}{\lambda_0 A_{eff}} \exp[2\int_0^z G(z')dz'], \\ d(z) = \frac{\lambda_0^2 D(z)}{4\pi c_l}. \quad (3)$$

## 3. THE PATH-AVERAGED MODEL

In this section, we briefly recall the derivation of the path-average model [28, 42] describing the change of the signal waveform over one compensation period. Equation (3) governing the $z$-evolution of an optical pulse can be written in the Hamiltonian form

$$i\frac{\partial A}{\partial z} = \frac{\delta H}{\delta A^*} = -d(z)A_{tt} - \epsilon c(z)|A|^2 A \quad (4)$$

with the Hamiltonian

$$H = \int \left\{ d(z)\,|A_t|^2 - \frac{\epsilon c(z)}{2}\,|A|^4 \right\} dt. \quad (5)$$

The true breathing soliton is a solution of Eq. (3) of the form

$$A(z,t) = \exp(ikz)F(z,t)$$

with a periodic function $F(z+Z_0,t) = F(z,t)$. It is interesting to find a systematic way to describe a family of periodic solutions $F$ with different quasi-momenta $k$. The basic idea suggested in [28] is to use the small parameter $\epsilon$ to derive a path-averaged model that gives a regular description of the breathing soliton in the leading order in $\epsilon$. Averaging cannot be performed directly in Eq. (1) in the case of large variations

$$\tilde{d} \gg \langle d \rangle,$$

where

$$d(z) = \tilde{d} + \langle d \rangle \quad \text{with} \quad \langle \tilde{d} \rangle = 0.$$

However, a path-averaged propagation equation can be obtained in the frequency domain [28]. We show that in some important limits, the averaged equation for the periodic breathing pulse can be transformed to the integrable NLS equation.

First, to eliminate the periodic dependence of the linear part, we follow [28] in applying the so-called Floquet–Lyapunov transformation

$$A_\omega = \phi_\omega \exp\{-i\omega^2 R(z)\}, \quad \frac{dR(z)}{dz} = d(z) - \langle d \rangle, \quad (6)$$

where $A_\omega = A(z,\omega)$ is the Fourier transform of

$$A(z,t) = \int A_\omega \exp[-i\omega t] d\omega.$$

An important observation used in what follows is that for a fixed amplitude of $d$, the amplitude of the variation of $R$ decreases as $m = Z_a/L$ increases. It can be easily found that

$$\max[R(z)] \propto 1/m.$$

In the new variables, the equation becomes

$$i\frac{\partial \phi_\omega}{\partial z} - \langle d \rangle \omega^2 \phi_\omega + \epsilon \int G_{\omega 123}(z)\delta(\omega + \omega_1 - \omega_2 - \omega_3) \times \\ \times \phi_1^* \phi_2 \phi_3 d\omega_1 d\omega_2 d\omega_3 = 0, \quad (7)$$

where

$$G_{\omega 123}(z) = c(z)\exp\{i\Delta\Omega R(z)\}$$

is $Z_a$-periodic and

$$\Delta\Omega = \omega^2 + \omega_1^2 - \omega_2^2 - \omega_3^2.$$

We note that $G_{\omega 123}$ depends only on the specific combination of the frequencies given by the resonance surface $\Delta\Omega$. Both the Fourier transform and Floquet–Lyapunov transform (6) are canonical and the transformed Hamiltonian $H$ is given by

$$H = \langle d \rangle \int \omega^2 |\phi_\omega|^2 d\omega - \varepsilon \int \frac{G_{\omega 123}}{2} \delta(\omega + \omega_1 - \omega_2 - \omega_3) \times \\ \times \phi_\omega^* \phi_1^* \phi_2 \phi_3 d\omega d\omega_1 d\omega_2 d\omega_3. \quad (8)$$

It is important that $\varepsilon$ and $\langle d \rangle$ are small, and Eq. (7) therefore has the so-called Bogolubov standard form and the averaging procedure can then be applied. We now apply the Hamiltonian averaging [50, 51]. We change the variables as

$$\phi_\omega = \varphi_\omega + \epsilon \int V_{\omega 123}\delta(\omega + \omega_1 - \omega_2 - \omega_3) \times \\ \times \varphi_1^* \varphi_2 \varphi_3 d\omega_1 d\omega_2 d\omega_3 + \dots,$$

where

$$V_{\omega 123}(z) = i\int_0^z [G_{\omega 123}(\tau) - T_{\omega 123}] d\tau + iV_{\omega 123}(0),$$

$$\langle V_{\omega 123} \rangle = 0$$

with

$$T_{\omega 123} = \langle G_{\omega 123} \rangle = \int_0^1 G_{\omega 123}(z) dz = \\ = \int_0^1 c(z)\exp\{i\Delta\Omega R(z)\} dz. \quad (9)$$

In the leading order in $\epsilon$, the path-averaged evolution of signal in the DM line is governed by the Gabitov–Turitsyn model [28]

$$i\frac{\partial \varphi_\omega}{\partial z} - \langle d \rangle \omega^2 \varphi_\omega + \epsilon \int T_{\omega 123}\delta(\omega + \omega_1 - \omega_2 - \omega_3) \times \\ \times \varphi_1^* \varphi_2 \varphi_3 d\omega_1 d\omega_2 d\omega_3 = 0. \quad (10)$$

The Hamiltonian averaging introduced here represents a regular way to calculate the next-order corrections to the averaged model. We note that Eq. (10) possesses a remarkable property. The matrix element $T_{\omega 123} = T(\Delta\Omega)$ is a function of $\Delta\Omega$ and on the resonant surface given by

$$\omega + \omega_1 - \omega_2 - \omega_3 = 0, \quad \Delta\Omega = \omega^2 + \omega_1^2 - \omega_2^2 - \omega_3^2 = 0,$$

both $T_{\omega 123}$ and its derivative with respect to $\Delta\Omega$ are regular. This observation allows us to make a quasi-identical transformation that eliminates the variable part of the matrix element $T_{\omega 123}$,

$$\varphi_\omega = a_\omega - \frac{\epsilon}{\langle d\rangle}\int \frac{T_0 - T_{\omega 123}}{\Delta\Omega} \times \\ \times a_1^* a_2 a_3 \delta(\omega+\omega_1-\omega_2-\omega_3) d\omega_1 d\omega_2 d\omega_3, \quad (11)$$

where $T_0 = T(0)$. This transformation has no singularities. If the integral part in this transformation is small compared to $a_\omega$, then in the leading order we obtain

$$i\frac{\partial a_\omega}{\partial z} - \langle d\rangle \omega^2 a_\omega + \epsilon \int T_0 \delta(\omega+\omega_1-\omega_2-\omega_3) \times \\ \times a_1^* a_2 a_3 d\omega_1 d\omega_2 d\omega_3 = 0. \quad (12)$$

This is nothing else but the integrable nonlinear Schrödinger equation written in the frequency domain. Obviously, this transformation is quasi-identical only if the integral in Eq. (11) is small compared to $a_\omega$. This is not true in the general case and that is why the path-averaged DM soliton given by the solution of Eq. (10) then has a form different from the cosh-shaped NLS equation soliton [28, 43, 49]. A comprehensive analysis of the DM soliton solutions of the Gabitov–Turitsyn equation has been published in [46–48]. The first high-precision numerical solution of the Gabitov–Turitsyn equation was presented in [48]. We note that if the kernel function in Eq. (11) is small,

$$|S(\Delta\Omega)| = \left|\frac{T_0 - T_{\omega 123}(\Delta\Omega)}{\Delta\Omega}\right| \ll 1, \quad (13)$$

then the averaged model can be reduced to the NLS equation. In other words, this is a condition on the functions $c(z)$ and $d(z)$ that makes the quasi-identical transformation possible. The path-averaged DM soliton propagation in systems satisfying requirement (13) is close to the dynamics of the traditional soliton and at the same time preserves all the advantages of the suppression of FWM by a high local dispersion.

## 4. SYSTEMS WITH A SHORT-SCALE MANAGEMENT

In this section, we calculate the matrix element $T_{\omega 123}$ for systems with a short-scale management ($L \ll Z_a$) and demonstrate that a path-averaged propagation (even with large variations of the dispersion) can be described by the integrable NLS equation in this regime. The matrix element $T$ plays an important role in the description of the FWM [52]. To be specific, we consider a two-step dispersion map with the amplification distance $Z_a = Z_0$ ($n = 1$) and dispersion compensation period $L = Z_a/m$ km. The dispersion is

$$d(z) = d + \langle d\rangle$$

if

$$\frac{k}{m} < \frac{z}{Z_a} < \frac{k+a}{m}$$

and

$$d(z) = \frac{da}{a-1} + \langle d\rangle$$

if

$$\frac{k+a}{m} < \frac{z}{Z_a} < \frac{k+1}{m},$$

where $k = 0, 1, 2, \ldots, m-1$ and the parameter $a \in (0,1)$ describes the position of the step. The mean-free function $R$ defined above can be found as

$$R(z) = d(z - Z_a k/m - aZ_a/(2m))$$

if

$$\frac{k}{m} < \frac{z}{Z_a} < \frac{k+a}{m}$$

and

$$R(z) = \frac{da}{a-1}\left[z - \frac{Z_a k}{m} - \frac{(a+1)Z_a}{2m}\right]$$

if

$$\frac{k+a}{m} < \frac{z}{Z_a} < \frac{k+1}{m}.$$

Straightforward calculations show that in this system, the matrix element $T_{\omega 123}$ is

$$T_{\omega 123} = \frac{\exp(2\gamma Z_a) - 1}{2\gamma Z_a \exp(2\gamma Z_a)}\left[1 + \frac{id\Delta\Omega}{2\gamma - id\Delta\Omega} \times \right. \\ \times \left[1 - \frac{2\gamma Z_a/m}{\exp(2\gamma Z_a/m) - 1} \times \right. \\ \left. \left. \times \frac{\exp\left[(2(1-a)\gamma + iad\Delta\Omega)Z_a/m\right] - 1}{(2(1-a)\gamma + iad\Delta\Omega)Z_a/m}\right]\right] \times \\ \times \exp\left[-iad\Delta\Omega\frac{Z_a}{2m}\right]. \quad (14)$$

To show a self-similar structure of this matrix element, we rewrite $T_{\omega 123}$ as

$$T_{\omega 123} = B(G)\cdot F(a, X, Y), \quad (15)$$

$$B(G) = \frac{G-1}{G\ln G}, \\ F(a,X,Y) = \left[1 + \frac{iY}{X - iY}\left[1 - \frac{X}{e^X - 1} \times \right.\right. \\ \left.\left. \times \frac{\exp[(1-a)X + iaY] - 1}{(1-a)X + iaY}\right]\right]\exp\left(-\frac{iaY}{2}\right), \quad (16)$$

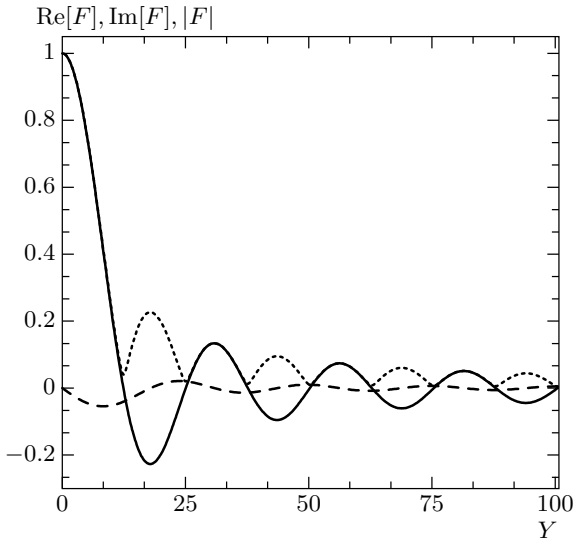


**Fig. 1.** Real (solid line) and imaginary (dashed line) parts and the absolute value (dotted line) of the function $F(a, X, Y)$ are plotted for $a = 0.5$ and $X = 0.63 \ln(10) dB$

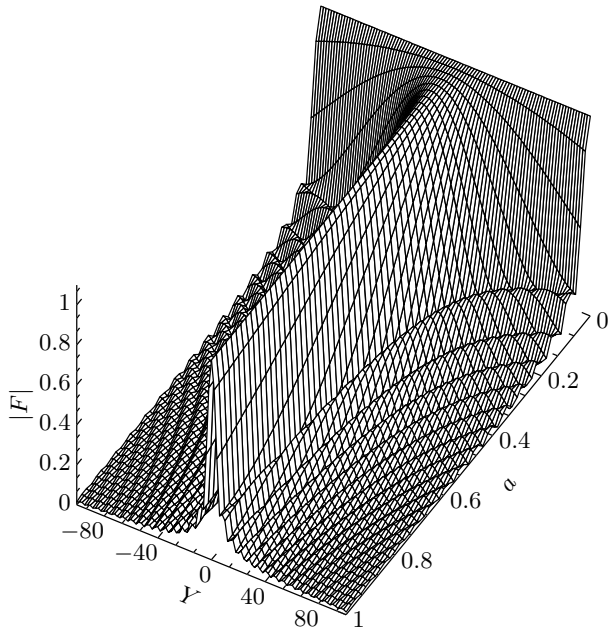


**Fig. 2.** The function $|F(a, X, Y)|$ versus $Y$ for the system with different $a$

where the amplitude $B$ is a function of only $G = \exp(2\gamma Z_a)$ and is independent of $m$. The shape $F(a, X, Y)$ is a function of the parameter $a$ and specific combinations of $X = 2\gamma Z_a/m$ and $Y = d\Delta\Omega Z_a/m$. The real part (solid line), the imaginary part (dashed line), and the absolute value (dotted line) of $F(a, X, Y)$ are plotted in Fig. 1. Here, $\alpha = 0.21$ dB/km, $Z_a = 60$ km, $m = 2$, and $a = 0.5$. Minima of the function $|F|$ correspond to operation regimes with the suppressed FWM [52]. In the $d = 0$ limit, we obviously recover results of the traditional path-averaged (guiding-center) soliton theory [24–26].

In Fig. 2, the function $|F(a, X, Y)|$ is plotted versus $Y$ for the different $a$ with the same parameters as in Fig. 1. We now estimate the matrix element of the quasi-identical transformation

$$|S(\Delta\Omega)| \le \left| \frac{1}{Z_a} \int_0^{Z_a} \frac{c(z)[\exp(i\Delta\Omega R(z)) - 1]}{\Delta\Omega} dz \right| \le$$

$$\le \max(R)\langle c \rangle = \frac{ad}{2m}\langle c \rangle.$$

It can be seen that as $m$ increases (with the other parameters fixed), the path-averaged model (10) governing the DM soliton propagation converges to the integrable NLS equation with

$$T(0) = \frac{G-1}{G \ln G}.$$

It is obvious that in the limit of a very weak loss (small $\gamma$), we again obtain the lossless model approximation for $T$,

$$T_{\omega 123} = \frac{\sin(aY)}{aY}.$$

However, the increase of $m$ (decrease of $L$) under the fixed characteristic bandwidth of the signal makes the oscillatory structure of the kernel insignificant. This implies that if $T(\Delta\Omega)$ is practically concentrated in some region, then the corresponding region in $\Delta\Omega$ is larger for large $m$ than for small $m$. For the pulses with the same spectral width, this means that $T$ is much flatter for large $m$: as a matter of fact, the function $T$ can be well approximated by the value $T(0)$ for large $m$ (small $L$). As a result, the NLS equation model works rather well in this limit and the solution (of the path-averaged model!) should be close to the cosh-like soliton of the NLS equation. We note that although it is known that the DM soliton shape is close to cosh for the lossless model in the so-called weak map ($S < 1$) limit [19, 28, 36, 34], this is not so obvious for a system with loss and different periods of the amplification and dispersion variations. In such a system, DM solitons therefore possess the dual advantages of being chirped (which is important for the suppression of the four-wave mixing in WDM systems) and of having the integrable path-averaged dynamics, which allows the use of well developed mathematical tools in studying prac-

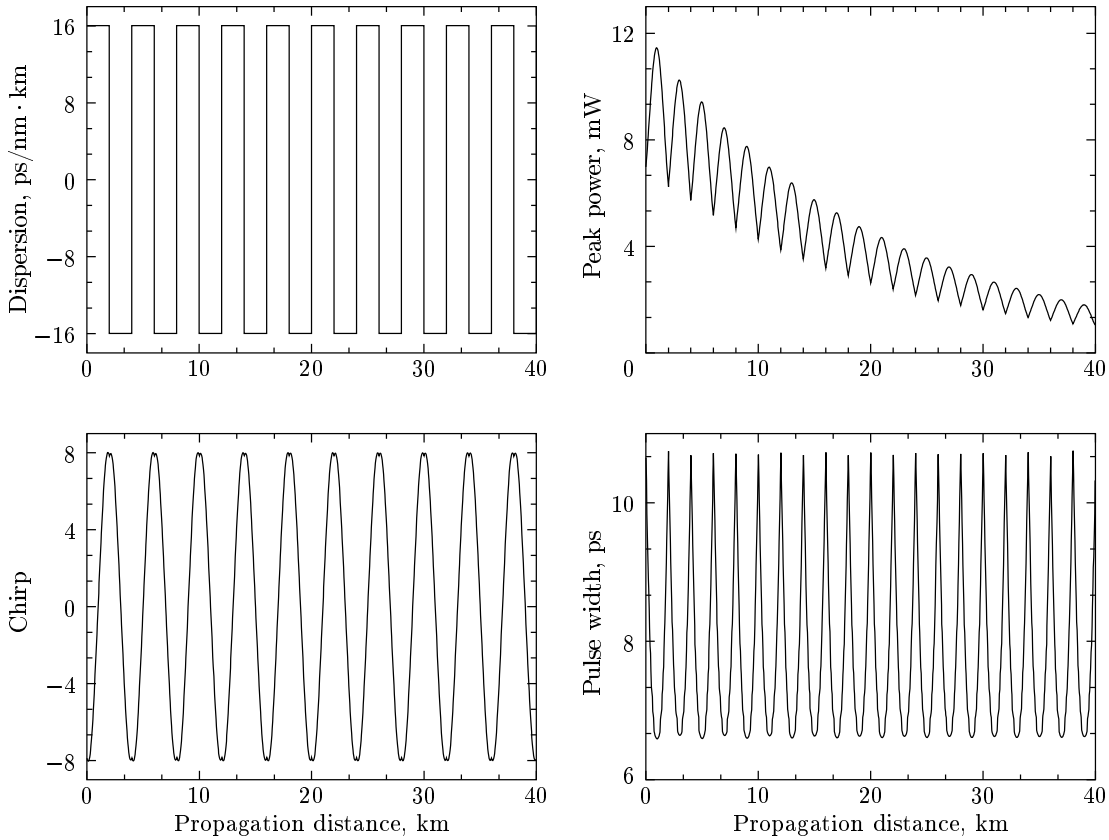


**Fig. 3.** Evolution of the soliton peak power (right top), chirp (left bottom), and full-width at half maximum (right bottom) along one section is shown for the transmission system with the short-scale dispersion map (left top). Here, $S = 2$, the amplification distance is 40 km, and the dispersion compensation period is 4 km

tical perturbations. This additionally implies that all the control techniques developed for the improvement of the traditional soliton transmission can be directly used in these systems.

## 5. A SINGLE PULSE PROPAGATION

In this section, we consider numerical simulation results for a single pulse propagation in systems with a short-scale management. In contrast to the lossless model, the evolution of soliton parameters over one period is here asymmetric because of the loss. Rapid variations of the pulse width, peak power, and chirp are accompanied by the exponential decay of the power due to the loss. Nevertheless, numerical simulations have revealed that there exists a true periodic solution that reproduces itself at the end of the compensation cell (in this case, at the end of the amplification period). For the DM soliton with the map strength $S = 2$, the evolutions of its peak power (right top), chirp (left bottom), and full width at half maximum (right bottom) along one section are shown in Fig. 3 for a transmission system with the short-scale dispersion map (left top). The amplification distance is 40 km and the dispersion compensation length is 4 km. The following parameters were used in the simulations: the dispersion in the two-step map $\pm 16 + 0.1$ ps/nm·km (see Fig. 3), the nonlinear coefficient $\sigma = 2\pi n_2/\lambda_0 A_{eff} = 2.43$ W$^{-1}$·km$^{-1}$, and the fiber loss $\alpha = 0.21$ dB/km.

The observed DM soliton is very stable and propagates without radiation as seen in Fig. 4 (where system parameters are the same as in Fig. 3). Figure 4 illustrates the chirp of the DM soliton versus the width. The left and right figures show this dependence for the first and the 140th sections, respectively.

An important feature of solitons in systems with a short-scale dispersion management is the reduced power. The DM soliton identified here has a reduced power compared to the previously studied DM soliton regimes ($L \geq Z_a$) for the same width propagating in a fiber system with the same average dispersion (with the

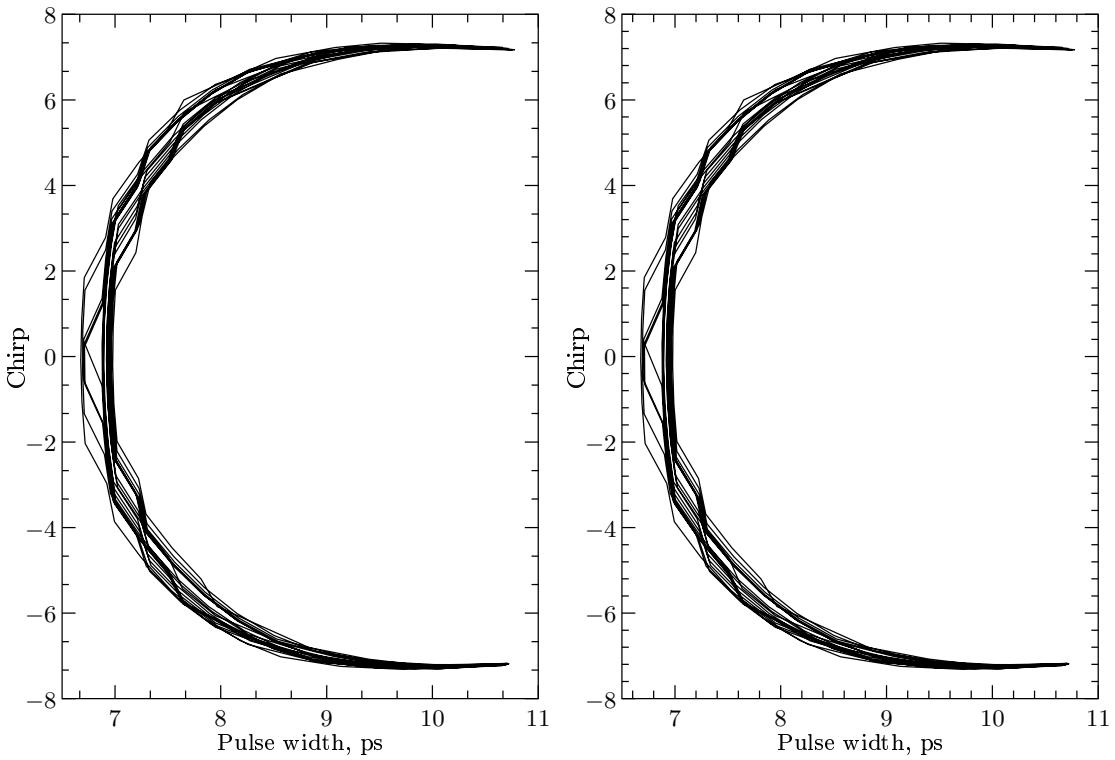


**Fig. 4.** Chirp versus width of the DM soliton for the first (left) and the 140th (right) sections

same parameters except the $L/Z_a$ ratio). This observation is illustrated by Fig. 5, where we present results of the modelling based on the zero-mode Gaussian approximation of the DM soliton (in the expansion using a complete basis of the chirped Gauss–Hermite functions, see [57] for details). Using this approach, we have built the evolution of the DM soliton peak power dependence on the pulse width; the dispersion compensation length was changed, but the average dispersion and the amplification distance were kept the same. In Fig. 5, the dependence of the DM soliton peak power on the pulse width at the beginning of the compensation section $z = 0$ is shown for different ratios of the dispersion period $L = Z_a/m$ to the amplification distance $Z_a$ (40 km here): $m = 10$ (solid line), 1 (long-dashed line), 0.5 (dashed line), 0.2 (dotted line), 0.1 (dashed-dotted line). For control, we also show the peak power dependence for the true DM soliton found numerically (in the full model) in the case where $m = 10$ (squares) and $m = 0.2$ (rhombuses).

We also note that the energy of the short-scale DM soliton is very close to that of the conventional soliton (although the pulse is chirped and experiences breathing oscillations of the width and chirp during propagation). This is because the effective map strength is here small due to small $L$. It is seen from Fig. 5 that the short-scale dispersion management ($m = 10$) indeed provides a reduced power of the DM soliton for the same pulse width (and the same average dispersion and the same other parameters except the ratio $L/Z_a$). Because the soliton power grows very rapidly with the reduction of the pulse width (after the curves in Fig. 5 pass some «critical» turning points, for instance, for $m = 1$ such a point is around 16 ps), this effect can be very important for high-bit-rate transmissions using short pulses.

## 6. SOLITON INTERACTION

The nonlinear pulse-to-pulse interaction is one the main limiting factors in the high-bit-rate optical data transmission. In this section, we present results on the soliton interaction in systems with a short-scale management with the amplification period $Z_a = 60$ km and the dispersion compensation period $L = 4$ km ($m = 15$), $L = 6$ km ($m = 10$), and $L = 12$ km ($m = 5$). Numerical simulations in this section include the third-order dispersion and Raman effects. An important advantage of operating close to the integrable limit (weak maps) discussed above is that the well developed tech-

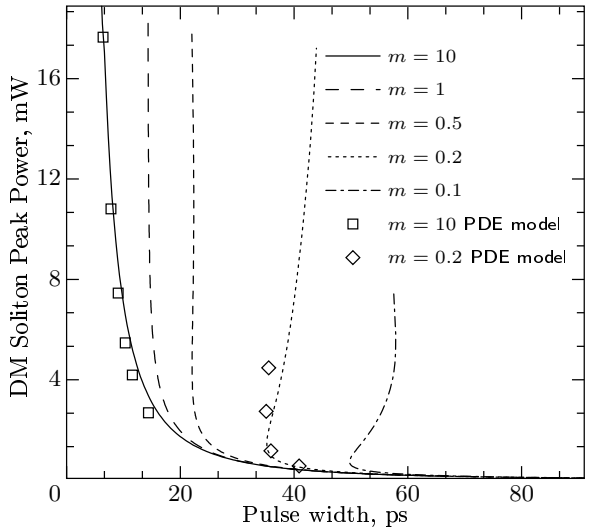


**Fig. 5.** The dependence of the DM soliton peak power on the pulse width at the beginning of the compensation section $z = 0$ for different ratios of the dispersion period $L = Z_a/m$ to the amplification distance $Z_a$: $m = 10$ (solid line), 1 (long-dashed line), 0.5 (dashed line), 0.2 (dotted line), and 0.1 (dashed-dotted line). The same dependences for the true DM soliton found numerically (in the full model) are shown for $m = 10$ (squares) and $m = 0.2$ (rhombuses)

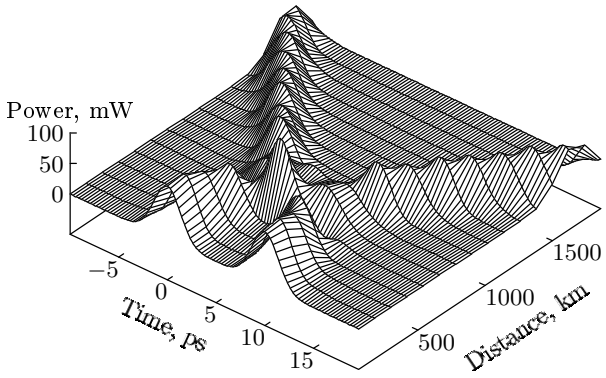


**Fig. 6.** The interaction of two in-phase DM solitons at 100 Gb/s. Here, $D = \pm 2.4 + 0.0785$ ps/nm·km, $Z_a = 60$ km, and $m = 15$; solitons with the peak power 5.44 mW and the pulse width 2.93 ps are launched at a chirp-free point located 0.56 km before the end of the section

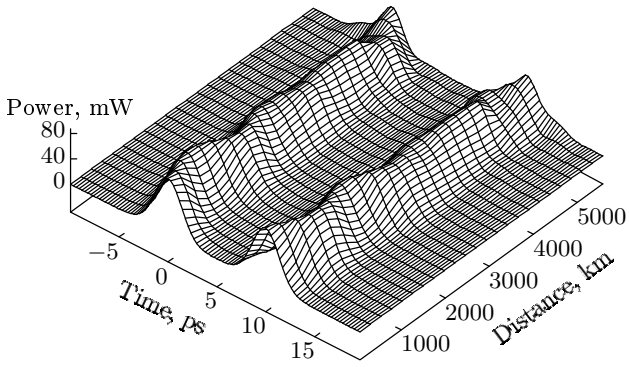


**Fig. 7.** The same as in Fig. 6 but with the initial phase alternation (out-of-phase solitons)

niques to suppress soliton interaction can be applied. Figures 6 and 7 show the effect of the initial phase alternation of neighboring solitons. Figure 6 shows the propagation of two in-phase solitons initially separated by 10 ps (100 Gb/s). The solitons collapse after approximately 500 km. In contrast, DM solitons with the initial phase shift $\pi$ can propagate over 5000 km without fusion. Here, $D = \pm 2.4 + 0.0785$ ps/nm·km, $Z_a = 60$ km, $m = 15$, the peak power of the single soliton is 5.44 mW, and the pulse width is 2.93 ps at the chirp-free point (0.56 km from the end of the map). We recall that the interaction of DM solitons with larger $S$ is independent of the initial phase shift [33].

Figure 8 shows the normalized distance between the Gaussian pulses for different initial phase shifts along the total distance $z = 1018.5$ km. The initial distance is $z = 12.5$ ps (80 Gb/s) and the maps are $D = \pm 1.6 + 0.04$ ps/nm·km, $D = \pm 2.4 + 0.04$ ps/nm·km, and $D = \pm 3.2 + 0.04$ ps/nm·km, with the respective strengths $S = 1.06$, 1.58, and 2.12. Figure 9 shows an improvement of the system performance resulting from the initial phase alternation. We plot the total transmission distance versus the DM soliton energy (at the beginning of the section) at 80 Gb/s. Here, the dispersion is $D = \pm 2.4 + 0.04$ ps/nm·km, $L = 6$ km, and $Z_a = 60$ km. The total transmission distance has been defined as the distance at which the $Q$ factor becomes less than 6 for two test random 128-bit patterns. The solid lines are for the initial signals with a phase alternation and dashed lines are for the in-phase input pulses. It can be seen that short-scale dispersion-managed systems are quite attractive candidates for the transmission optical data at ultra-high-bit rates. Optimization of such lines will lead to a further improvement of the system performance.

## 7. CONCLUSIONS

We have identified a stable optical pulse propagation regime in fiber systems with the short-scale

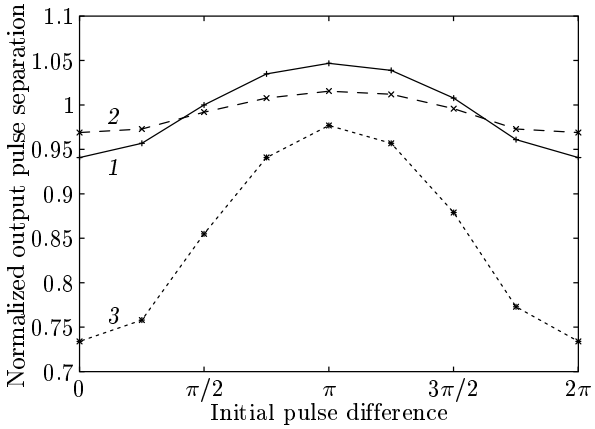


**Fig. 8.** The normalized pulse separation versus the initial phase shift (the total distance $z = 1018.5$ km) for different map strengths: $S = 1.06$ (solid line *1*), $S = 1.58$ (long-dashed line *2*), and $S = 2.12$ (dashed line *3*). Here, $Z_a = 60$ km and $L = 6$ km

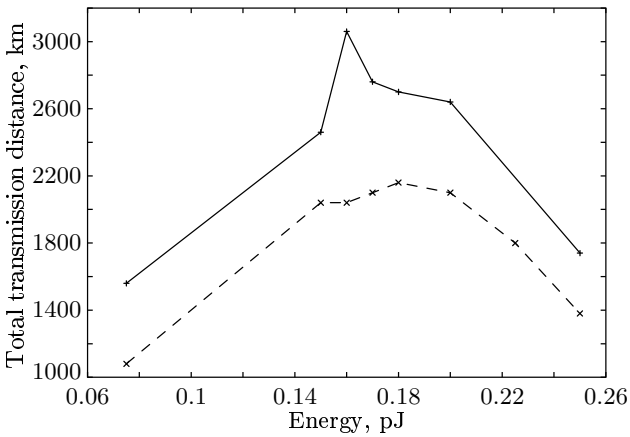


**Fig. 9.** The transmission distance at $80Gb/s$ with (solid line) and without (dashed line) the initial phase alternation versus the DM soliton energy. Here, $D = \pm 2.4 + 0.04$ ps/nm·km, $L = 6$ km, and $Z_a = 60$ km

dispersion management when the compensation period is much shorter than the amplification distance. In systems with a short-scale management, the DM soliton has a reduced power compared to the usual DM soliton ($L > Z_a$) of the same width (and the same amplification distance and average dispersion). The short-scale management is a means of controlling the strength of the map (and consequently, pulse energy, interactions, etc.) while keeping the average dispersion finite and taking advantage of the FWM suppression in WDM by a high local dispersion. We show that the path-averaged dynamics of chirped DM solitons in systems with a short-scale management for weak maps is close to that in the integrable model. Therefore, DM solitons in such systems possess the dual advantages of being chirped (which is important for the suppression of the four-wave mixing in WDM systems) and of possessing the integrable path-averaged dynamics, which allows the use of well developed mathematical tools for studying practical perturbations.

We would like to thank S. K. Turitsyn for useful discussions. The support of EPRSC and RFBR (grant 99-02-16688) is acknowledged.

## REFERENCES


1. A. Hasegawa and F. D. Tappert, Appl. Phys. Lett. **23**, 142 (1973).
2. V. E. Zakharov and A. B. Shabat, Zh. Eksp. Teor. Fiz. **60**, 136 (1971).
3. S. V. Manakov, Zh. Ekp. Teor. Fiz. **65**, 505 (1973).
4. L. F. Mollenauer, R. H. Stolen, and J. P. Gordon, Phys. Rev. Lett. **45**, 1095 (1980).
5. L. F. Mollenauer and K. Smith, Opt. Lett. **13**, 675 (1988).
6. V. E. Zakharov, S. V. Manakov, S. P. Novikov, and L. I. Pitaevskii, *The Theory of Solitons. The Inverse Transform Method*, Nauka, Moscow (1980).
7. A. C. Newell and J. V. Moloney, *Nonlinear Optics*, Addison-Wesley Publishing Company, Redwood City CA (1992).
8. M. J. Ablowitz and P. A. Clarkson, *Solitons, Nonlinear Evolution Equations, and Inverse Scattering*, Cambridge University Press, Cambridge, UK (1991).
9. A. Hasegawa and Y. Kodama, *Solitons In Optical Communications*, Clarendon, Oxford (1995).
10. R. K. Dodd, J. C. Eilbeck, J. D. Gibbon, and H. C. Morris, *Solitons and Nonlinear Wave Equations*, Academic Press, New York (1984).
11. M. J. Ablowitz, D. J. Kaup, A. C. Newell, and H. Segur, Stud. Appl. Math. **53**, 294 (1974).
12. E. A. Kuznetsov, A. M. Rubenchik, and V. E. Zakharov, Phys. Rep. **142**, 103 (1986).
13. L. F. Mollenauer, P. V. Mamyshev, and M. J. Neubelt, Post Deadline Presentation, PD22-1, OFC'96, San Jose (1996).

**14**. *Optical Fiber Telecommunications III A*, ed. by I. P. Kaminow and T. L. Koch, Academic Press (1997), v. IIIA.

**15**. F. M. Knox, W. Forysiak, and N. J. Doran, IEEE J. Lightwave Technol. **13**, 1955 (1995).

**16**. M. Suzuki, I. Morita, N. Edagawa, S. Yamamoto, H. Taga, and S. Akiba, Electron. Lett. **31**, 2027 (1995).

**17**. M. Nakazawa and H. Kubota, Electron. Lett. **31**, 216 (1995).

**18**. H. A. Haus, K. Tamura, L. E. Nelson, and E. P. Ippen, IEEE J. Quant. Electr. **31**, 591 (1995).

**19**. N. Smith, F. M. Knox, N. J. Doran, K. J. Blow, and I. Bennion, Electron. Lett. **32**, 54 (1996).

**20**. M. Nakazawa, H. Kubota, A. Sahara, and K. Tamura, IEEE Photon. Technol. Lett. **8**, 452 (1996).

**21**. M. Nakazawa, K. Suzuki, H. Kubota, and E. Yamada, Electron. Lett. **32**, 1686 (1996).

**22**. M. Suzuki, I. Morita, K. Tanaka, N. Edagawa, S. Yamamoto, and S. Akiba, ECOC'97, Edinburgh (1997), Vol. **3**, p. 99.

**23**. D. Le Guen, F. Favre, M. L. Moulinard, M. Henry, F. Devaux, and T. Georges, ECOC'97, Edinburgh (1997), Postdeadline Paper, Vol. **5**, p. 25.

**24**. L. F. Mollenauer, S. G. Evangelides Jr., and H. A. Haus, IEEE J. Lightwave Tech. **9**, 194 (1991).

**25**. A. Hasegawa and Y. Kodama, Opt. Lett. **15**, 1443 (1990); Phys. Rev. Lett. **66**, 161 (1991).

**26**. K. J. Blow and N. J. Doran, IEEE Photon. Technol. Lett. **3**, 369 (1991).

**27**. A. F. Evans, in *Optical Fiber Communication Conference*, 1998, OSA Technical Digest Series, OSA, Washington, D.C. (1998), Vol. 2, p. 22.

**28**. I. Gabitov and S. K. Turitsyn, Opt. Lett. **21**, 327 (1996).

**29**. N. J. Smith, N. J. Doran, F. M. Knox, and W. Forysiak, Opt. Lett. **21**, 1981 (1997).

**30**. T. Georges and B. Charbonnier, IEEE Photon. Techn. Lett. **9**, 127 (1997).

**31**. J. M. Jacob, E. A. Golovchenko, A. N. Pilipetskii, G. M. Carter, and C. R. Menyuk, IEEE Photon. Technol. Lett. **9**, 130 (1997).

**32**. M. Matsumoto and H. A. Haus, IEEE Photon. Technol. Lett. **9**, 785 (1997).

**33**. E. A. Golovchenko, A. N. Pilipetskii, and C. R. Menyuk, Opt. Lett. **22**, 793 (1997).

**34**. T. S. Yang and W. L. Kath, Opt. Lett. **22**, 985 (1997).

**35**. D. Breuer, F. Kueppers, A. Mattheus, E. G. Shapiro, I. Gabitov, and S. K. Turitsyn, Opt. Lett. **22**, 546 (1997).

**36**. J. H. B. Nijhof, N. J. Doran, W. Forysiak, and F. M. Knox, Electron. Lett. **33**, 1726 (1997).

**37**. V. S. Grigoryan, T. Yu, E. A. Golovchenko, C. R. Menyuk, and A. N. Pilipetskii, Opt. Lett. **22**, 1609 (1997).

**38**. A. Sahara, H. Kubota, and M. Nakazawa, IEEE Photon. Techn. Lett. **9**, 1179 (1997).

**39**. S. Kumar and A. Hasegawa, Opt. Lett. **22**, 372 (1997).

**40**. A. Hasegawa, Y. Kodama, and A. Maruta, Opt. Fiber Techn. **3**, 197 (1997).

**41**. S. K. Turitsyn, M. Fedoruk, and A. Gornakova, Opt. Lett. **24**, 869 (1999).

**42**. S. B. Medvedev and S. K. Turitsyn, Pis'ma v Zh. Eksp. Teor. Fiz. **69**, 465 (1999).

**43**. M. J. Ablowitz and G. Biondini, Opt. Lett. **23**, 1668 (1998).

**44**. S. K. Turitsyn and V. K. Mezentsev, Pis'ma v Zh. Eksp. Teor. Fiz. **68**, 830 (1998).

**45**. V. E. Zakharov and S. V. Manakov, Pis'ma v Zh. Eksp. Teor. Fiz. **70**, 573 (1999).

**46**. P. M. Lushnikov, Opt. Lett. **25**, 1144 (2000).

**47**. D. E. Pelinovsky, Phys. Rev. E **62**, 4283 (1998).

**48**. P. M. Lushnikov, Opt. Lett. **26**, 1535 (2001).

**49**. V. E. Zakharov, in *Optical Solitons. Theoretical Challenges and Industrial Perspectives*, ed. by V. E. Zakharov and S. Wabnitz, Springer, EDP Sciences (1999).

**50**. V. I. Arnold, *Geometrical Methods in the Theory of Ordinary Differential Equations*, Springer-Verlag, New York (1988).

**51**. V. E. Zakharov, V. S. L'vov, and G. Falkovich, *Kolmogorov Spectra of Turbulence*, Springer-Verlag, Berlin (1992).

**52**. S. K. Burtsev and I. Gabitov, in *Proc. of II Intern. Symp. on Physics and Applications of Optical Solitons in Fibers*, Kyoto (1997), Kluwer, Dordrecht (1998), p. 261.

**53**. J. N. Kutz, P. Holmes, S. G. Evangelides Jr., and J. P. Gordon, JOSA B **15**, 87 (1998).

**54**. S. K. Turitsyn and E. G. Shapiro, Opt. Fiber Techn. **4**, 151 (1998).

**55**. D. S. Govan, W. Forysiak, and N. J. Doran, Opt. Lett. **23**, 1523 (1998).

**56**. N. S. Bergano, C. Davidson, M. Ma, A. Pilipetskii, S. Evangelides, H. Kidorf, J. Darcie, E. Golovchenko, K. Rottwitt, P. Corbett, R. Menges, M. Mils, B. Pedersen, D. Peckham, A. Abramov, and A. Vengsarkar, Post Deadline Presentation, PD12-1, OFC'98, San Jose, USA (1998).

**57**. S. K. Turitsyn, E. G. Shapiro, and V. K. Mezentsev, Opt. Fiber Techn. **4**, 384 (1998).